

## N-dimensional dynamical systems exploiting instabilities in full

J. Rius, M. Figueras, R. Herrero, J. Farjas, F. Pi et al.

Citation: *Chaos* **10**, 760 (2000); doi: 10.1063/1.1324650

View online: <http://dx.doi.org/10.1063/1.1324650>

View Table of Contents: <http://chaos.aip.org/resource/1/CHAOEH/v10/i4>

Published by the [American Institute of Physics](#).

---

### Additional information on Chaos

Journal Homepage: <http://chaos.aip.org/>

Journal Information: [http://chaos.aip.org/about/about\\_the\\_journal](http://chaos.aip.org/about/about_the_journal)

Top downloads: [http://chaos.aip.org/features/most\\_downloaded](http://chaos.aip.org/features/most_downloaded)

Information for Authors: <http://chaos.aip.org/authors>

### ADVERTISEMENT

AIP Advances

The logo for AIP Advances, featuring the text 'AIP Advances' in a blue and green font. Above the text is a decorative arc of orange circles of varying sizes.

*Submit Now*

**Explore AIP's new  
open-access journal**

- **Article-level metrics  
now available**
- **Join the conversation!  
Rate & comment on articles**

# ***N*-dimensional dynamical systems exploiting instabilities in full**

J. Rius and M. Figueras

*Departament de Física, Universitat Autònoma de Barcelona, 08193 Bellaterra, Spain*

R. Herrero

*Departament de Mecànica de Fluids, Termodinàmica i Física, EUETIB, Universitat Politècnica de Catalunya, Comte d'Urgell, 187, 08036 Barcelona, Spain*

J. Farjas

*Departament de Física, Universitat de Girona, Avinguda Santaló, s/n, 17071 Girona, Spain*

F. Pi and G. Orriols

*Departament de Física, Universitat Autònoma de Barcelona, 08193 Bellaterra, Spain*

(Received 31 May 2000; accepted for publication 21 September 2000)

We report experimental and numerical results showing how certain  $N$ -dimensional dynamical systems are able to exhibit complex time evolutions based on the nonlinear combination of  $N-1$  oscillation modes. The experiments have been done with a family of thermo-optical systems of effective dynamical dimension varying from 1 to 6. The corresponding mathematical model is an  $N$ -dimensional vector field based on a scalar-valued nonlinear function of a single variable that is a linear combination of all the dynamic variables. We show how the complex evolutions appear associated with the occurrence of successive Hopf bifurcations in a saddle-node pair of fixed points up to exhaust their instability capabilities in  $N$  dimensions. For this reason the observed phenomenon is denoted as the full instability behavior of the dynamical system. The process through which the attractor responsible for the observed time evolution is formed may be rather complex and difficult to characterize. Nevertheless, the well-organized structure of the time signals suggests some generic mechanism of nonlinear mode mixing that we associate with the cluster of invariant sets emerging from the pair of fixed points and with the influence of the neighboring saddle sets on the flow nearby the attractor. The generation of invariant tori is likely during the full instability development and the global process may be considered as a generalized Landau scenario for the emergence of irregular and complex behavior through the nonlinear superposition of oscillatory motions. © 2000 American Institute of Physics. [S1054-1500(00)01004-1]

**Oscillatory phenomena are ubiquitous in natural and social systems and their investigation is currently done within the context of nonlinear dynamics. The oscillations in a given system may appear associated either with intrinsically sustained mechanisms or with externally modulated inputs. Processes with different time scales often coexist and in certain cases the interrelation of oscillations produces complex evolutions in which, however, cyclic repetitions are usually apparent. For instance, in biology, a direct example of this behavior is found in the bursting response of small neural networks in the stomatogastric nervous system of crustacea,<sup>1</sup> while a more involved example could be the wake–sleep cycle of a brain. Leaving apart the case of external modulations, we find it interesting to understand how a nonlinear system can produce different characteristic frequencies and how it can mix the corresponding oscillations to yield complex time evolutions. Although the problem looks basic and simple its answer is pending. The paradigm of chaos is not useful here and among the known mechanisms of nonlinear dynamics only the Landau scenario can be invoked. The present work is a contribution to the enlightenment of this problem. We report experimental and numerical results showing the emergence of complexity**

**through the nonlinear superposition of oscillatory motions in a dynamical system. The phenomenon develops in a generalized Landau scenario where the oscillations appear in association with the Hopf bifurcations of a set of fixed points and the complexity arises from (i) the number of different characteristic frequencies, and (ii) the variety of forms through which the nonlinear mechanisms combine the oscillation modes. The phenomenon is relevant because it illustrates how the nonlinear mode mixing works in nonlinear dynamics and it would probably be involved in any system exhibiting various self-sustained oscillations simultaneously.**

## **I. INTRODUCTION**

Complexity may emerge through a variety of ways in nonlinear dynamics although it is mostly associated with the irregularity of chaos. The peculiar properties of the chaotic states<sup>2</sup> are compatible with a low number of degrees of freedom, while additional levels of complex dynamics can be introduced in high-dimensional systems by properly augmenting the structure of the nonlinear part of the vector field. For instance, the effective participation of more dynamical variables within the nonlinear feedback may enhance the in-

stability capabilities of the fixed points and other limit sets. This article considers a situation of this type and presents experimental and numerical results showing the emergence of complex time dynamics independently of chaos.

The problem we are dealing with is how a large number of characteristic frequencies can successively appear in the system response and how the corresponding oscillations can mix to yield complex time evolutions. The theory of bifurcations shows that the exclusive way for introducing characteristic frequencies into the time dynamics is through the variety of Hopf-type two-dimensional instabilities,<sup>2</sup> i.e., the Poincaré-Andronov-Hopf bifurcation of a fixed point, the Naimark-Sacker or secondary Hopf bifurcation of a limit cycle, and the successive bifurcations originating higher-order invariant tori. This relates our problem to the Landau proposal<sup>3</sup> for tentatively explaining the emergence of turbulence through an indefinite sequence of oscillatory instabilities that, in light of the bifurcation theory, is usually associated with a sequence of torus bifurcations.<sup>4</sup> The Landau sequence is not considered a route to chaos because it does not produce sensitivity to initial conditions<sup>5</sup> and this is in strong contrast with the already existing strange attractors when triply periodic flows on three-dimensional tori are perturbed.<sup>6</sup> On the other hand, the lack of dissipative systems exhibiting such large sequences of torus bifurcations has left the Landau scenario as a hypothetical way for incorporating additional degrees of freedom into the oscillatory dynamics of high-dimensional systems.

This work shows that the combination of oscillatory motions in a nonlinear dynamical system can effectively yield complex time evolutions evoking the Landau idea about the emergence of irregularity. This behavior has been found in systems able to exploit all the instability capabilities of their fixed points through Hopf bifurcations. In relation to the Landau scenario, our problem is simpler because it deals with systems of finite dimension, but it is enriched by considering (i) more than one fixed point and (ii) the occurrence of successive Hopf bifurcations on each fixed point. The former is relevant because the nonlinear mechanisms can mix the oscillatory dynamics emerging from neighboring points, while the latter implies a variety of coexisting limit cycles and the possibility of different sequences of torus bifurcations. Nevertheless, as it will be shown, the complex time evolutions observed under these circumstances cannot be explained by means of the torus bifurcations alone and more general and more robust mechanisms of nonlinear mode mixing must be invoked.

More concretely, we deal with *N*-dimensional dynamical systems possessing a nonlinear function of a single variable that, in its turn, is a linear combination of the *N* dynamical variables. The fixed points of these systems appear aligned in phase space in an alternate sequence of saddle-node type. The saddle separatrices determine the attraction basins of the nodes and the basic dynamical phenomena will be associated with an attractor arising from one of the nodes and growing under the influence of the nearest saddle point. In *N* dimensions, a saddle-node pair of fixed points can sustain a total of *N*-1 Hopf bifurcations, occurring on either one or the other point,<sup>7</sup> and affecting differently oriented planes of the phase

space. The points initially have stable manifolds of dimension *N*-1 and *N*, respectively, and after the *N*-1 bifurcations one of them has become fully unstable while the other possesses only one stable dimension. *N*-1 limit cycles have successively emerged from the points and some invariant tori could have been created through secondary Hopf bifurcations of the cycles.<sup>8</sup> The cluster of limit sets contains an attractor at least<sup>9</sup> and a variety of saddles with the common feature of having a branch of their unstable manifold ending toward the attractor. The secondary processes occurring under such circumstances may be rather complex, but the experimental and numerical results show that they produce the nonlinear mixing of oscillation modes with relatively generic features. In essence, the attractor incorporates localized helical motions related to the influence of the neighboring saddles and, in this way, the observed time dynamics describes an irregular succession of oscillatory trains based on the *N*-1 characteristic frequencies initially generated from the pair of fixed points. We call the exhibition of such complex time waveforms the full instability behavior of the *N*-dimensional system and a detailed analysis of such behavior within a more general context has been presented in a separate paper.<sup>10</sup> Our aim here is to demonstrate the full instability behavior with a family of physical devices whose effective dynamical dimension may easily be varied and we describe experimental results for successively increasing dimensions up to *N*=6. The interpretation is sustained with the linear stability analysis and numerical simulations of a mathematical model reproducing correctly the experimental results.

## II. NONLINEAR SYSTEM

The nonlinear systems are based on the so-called optothermal bistability with localized absorption (BOITAL)<sup>11</sup> and they have been described in detail elsewhere from both the experimental<sup>12</sup> and mathematical<sup>13,14</sup> points of view. A BOITAL device consists of a Fabry-Pérot cavity in which the input mirror is partially absorbing and the spacer is a multilayer of transparent materials with alternatively opposite thermo-optic effects. Concretely, in this work we used layers of glass, sunflower oil, silicone (F600, Bayer AG), optical adhesive (NOA61, Norland), and optical gel (0608, Cargille) with thicknesses ranging from  $\mu\text{m}$  to mm. Thermal expansion works in the case of glass as a positive phase-shifting effect ( $10^{-5} \text{ K}^{-1}$ ) while the rest of the materials produce negative shifting effects due to refractive index changes ( $-2$  to  $-5 \times 10^{-4} \text{ K}^{-1}$ ). The cavity mirrors were a high reflection ( $>0.98$ ) dielectric multilayer and a 7 nm nickel-chrome film having reflections of about 0.2 and transmission of about 0.4. The device was placed on a thermoelectric plate to define better the environment temperature and was irradiated for the metal mirror side with a laser beam of 514.5 nm wavelength focused to a 0.3 mm diameter spot. The reflected light was detected by means of a photodiode and a signal proportional to the reflected power,  $P_R$ , was digitized and stored in a computer. The incident laser power,  $P_E$ , was used as the control parameter.

The time dynamics in BOITAL devices is associated

with the heat propagation from the absorbing mirror through the cavity spacer, while the light provides an instantaneous nonlinear feedback to the heat source. The light wave tests the spacer temperature by means of its phase shift in a cavity round-trip and transfers such information to the absorbing mirror by means of interference effects. The temperature distribution remains practically unchanged during the light round-trip and determines therefore the interference state at that time. On the other hand, the light interference depends nonlinearly on the phase shift through the Airy function of the cavity and it constitutes the exclusive nonlinearity of the system. In addition, the multilayer of alternatively opposite thermo-optic materials can originate oscillatory instabilities because (i) the temperature variations produce competitive contributions to the light phase shift and, (ii) such contributions are time delayed according to the relative position of the layers with respect to the absorbing mirror. With a proper choice of materials and thicknesses, the various spacing layers behave as effective degrees of freedom and the number of layers determines the dynamical dimension of the system.

Some materials, like the adhesives and gels, exhibit significant and opposite phase-shifting effects due to both expansion and refraction, and usually these effects have really different time constants. Under proper circumstances, a single layer of one of such materials can introduce two effective degrees of freedom into the system dynamics and higher dimensionalities may be experimentally achieved in this way. This behavior has been known since the first optical bistability experiments on self-sustained oscillations in semiconductors<sup>15</sup> and more recently for the case of an optical adhesive.<sup>16</sup> On the other hand, the phase-shifting coefficients of these materials exhibit a significant temperature dependence that can be used for a fine adjustment of the spacer structure by means of the environment temperature regulation.

The physical description of a BOITAL system is based on the homogeneous heat equation subject to the proper continuity and boundary conditions, of which the one describing the localized heat source by light absorption is nonlocal and nonlinear.<sup>13</sup> The linear stability analysis of the stationary solution points out clearly an effective dynamical dimension equal to the number of spacing layers and it has been shown that the partial differential equation may be reduced to the following dimensionless low-order model:<sup>14</sup>

$$\frac{d\psi_j}{dt} = - \sum_{i=1}^N b_{ji}(\psi_i - a_i A(\psi)\mu_E), \quad j=1,2,\dots,N, \quad (1a)$$

with

$$\psi = \psi^0 + \sum_1^N \psi_j, \quad (1b)$$

where  $\psi$  is the round-trip phase shift and  $\psi^0$  is its value in the absence of laser heating.  $N$  is the number of layers and each variable  $\psi_j$  denotes the variation due to temperature changes of the phase shift associated with the  $j$ th layer.  $\psi_j$  is proportional to the space-averaged temperature across the layer and to the thermo-optic coefficient of the corresponding material. The parameters  $b_{ji}$  and  $a_i$  depend on the cavity

spacer properties and thermal boundary conditions,<sup>14</sup> and  $\mu_E$  is the incident light intensity normalized in such a way that  $\sum a_i = 1$ . The rates  $b_{ji}$  describe the thermal coupling between layers and the associated diffusion times, while  $a_j$  characterizes the effective contribution of the  $j$ th layer to the phase shift variations.  $A(\psi)$  describes the light interference within the absorbing film and it is a positive-defined almost-sinusoidal function depending only on the mirror parameters.<sup>13</sup> It may be written in the following closed form:

$$A(\psi) = \frac{\mu_1 \cos \psi - \mu_2}{\cos \psi - \mu_3}, \quad (2)$$

very convenient for the numerical simulations, and the results reported in the paper correspond to  $\mu_1 = 1.06$ ,  $\mu_2 = 1.25$ , and  $\mu_3 = 1.86$ . The reflected light intensity is given by  $R(\psi)\mu_E$ , with the interferometer reflection  $R(\psi) \simeq 1 - A(\psi)$ . The  $\psi(t)$  evolution will typically present variations larger than  $2\pi$  and supplementary foldings appear then in the reflected power signal. Such foldings simply describe the phase shift overcoming the maximum or minimum reflection values and lack of dynamical significance (see, e.g., Fig. 2).

It is useful to know that the system (1) admits to being linearly transformed to a canonical form as follows:<sup>14</sup>

$$\begin{aligned} \dot{x}_1 &= - \sum_{j=1}^N c_j x_j + A(\psi)\mu_E, \\ \dot{x}_j &= x_{j-1}, \quad j=2, \dots, N, \end{aligned} \quad (3a)$$

with

$$\psi = \psi^0 + \sum_{j=1}^N d_j x_j, \quad (3b)$$

where the coefficients  $c_q$  and  $d_q$  are functions of the  $b_{ji}$  and  $a_i$  and, in particular,  $d_N = c_N$ . For cavity spacers of alternatively opposite thermo-optic materials, the corresponding set of  $d_j$  values present alternatively opposite signs. The new variables lack of direct physical interpretation, but the simplicity of the canonical form facilitates the analysis and the comparison with other models. In addition, we have shown<sup>10</sup> that the linear stability analysis of (3) can be used to design  $N$ -dimensional systems, i.e., to determine their  $c_j$  and  $d_j$  values, in which the fixed points of a saddle-node pair experience  $N-1$  Hopf bifurcations with preselected values for the oscillation frequency and control parameter. The numerical simulations reported in this paper correspond to systems designed with this method.

The steady-state solution of Eqs. (1) or (3) as a function of  $\mu_E$  is determined by  $A(\psi)$  and consists of successive S-shaped branches. BOITAL devices with different spacer structures but equal mirrors have the same steady-state branching diagram describing  $\psi$  vs  $\mu_E$ . The properties of the cavity spacer determine the power scale factor of the bifurcation diagram through the normalization factor included in  $\mu_E$  and, most importantly, the possibility of oscillatory instabilities on the steady-state branches.<sup>13,14</sup>

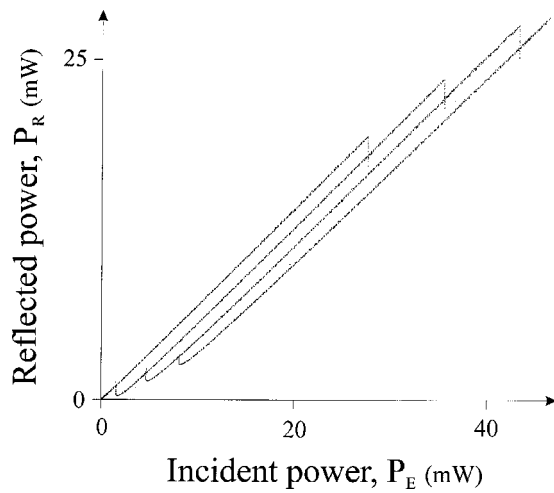


FIG. 1. Reflected light power as a function of the incident power for a BOITAL cavity spaced with 200  $\mu\text{m}$  of sunflower oil.

### III. DYNAMICAL PHENOMENA FOR SUCCESSIVELY INCREASING DIMENSION

The BOITAL family enables us to analyze systems of successively increasing dimension for the gradual understanding of complex time evolutions. With this aim we begin by briefly describing known results for  $N=1, 2,$  and  $3,$  and then present experimental results for  $N=4$  and  $6,$  and numerical simulations for  $N=6$  and  $10.$

Figure 1 shows the response of a BOITAL cavity spaced with a single material.<sup>11</sup> It represents the reflected light power when the incident power is slowly varied with successive back and forth sweepings. The device exhibits switching jumps and the consequent hysteresis cycles associated with pairs of saddle-node bifurcations. The saddle solution in between two stable branches plays in this case the simple role of a separatrix in a one-dimensional phase space.

The presence of a second material with opposite thermo-optic effect within the cavity results in proper dynamical phenomena of two-dimensional phase spaces.<sup>17</sup> The bifurcation diagram is also formed by successive hysteresis cycles but, in addition, it contains oscillatory states that appear and disappear by means of a Hopf bifurcation occurring two times on each node branch. Near the Hopf bifurcation the frequency is the same in all the branches but the oscillations may suffer the influence of a neighboring saddle point when the limit cycle grows. As shown in the example of Fig. 2, the oscillation period strongly increases until the orbit makes tangency to the saddle and vanishes in a homoclinic bifurcation, after which the system evolves toward the oscillatory state emerging from the node point located at the other side of the saddle separatrix.

Figure 3 shows the three basic kinds of three-dimensional dynamics observed in the response of BOITAL cavities.<sup>12,18</sup> The stable limit cycle born in the Hopf bifurcation of a node point passes near a saddle limit set that now may be either a saddle focus with inward spiraling [Fig. 3(a)] or a saddle limit cycle generated by a Hopf bifurcation of that point [Fig. 3(b)]. In this way, the time evolution of the attractor incorporates the faster oscillation frequency associ-

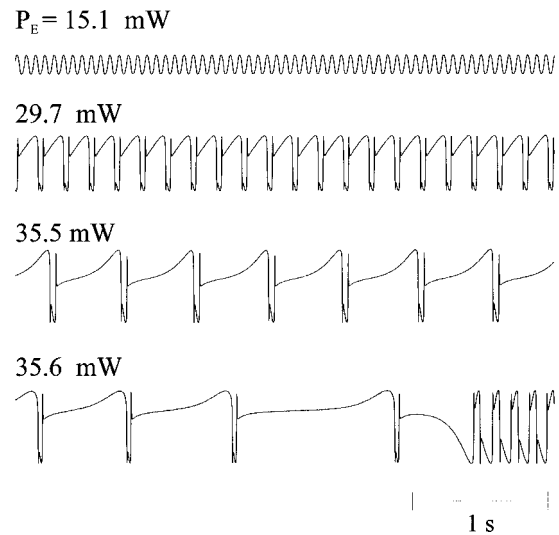


FIG. 2. Time evolution of the reflected power for different incident powers observed in a two-layer device spaced with 140 and 75  $\mu\text{m}$  of glass and sunflower oil, respectively. The vertical scale in arbitrary units is the same for all the recordings. The lower signal is a transient indicating the occurrence of a homoclinic bifurcation in between 35.5 and 35.6 mW. The interferometric foldings in the reflected power signals denote phase shift variations larger than  $2\pi$  and have no dynamical significance.

ated with the saddle limit set, and the nearer the attractor passes to the saddle the larger the number of fast oscillations. In the third kind of dynamics [Fig. 3(c)], the stable limit cycle bends by reinjecting toward the inner point from which it originated and which now is a saddle focus with outward spiraling. The reinjection bending is related to a distant and large saddle limit cycle and the fast reinjection peak denotes the characteristic time of that cycle. When the incident power is increased, the attractor grows and the approach to the external saddle cycle produces a higher number of successive

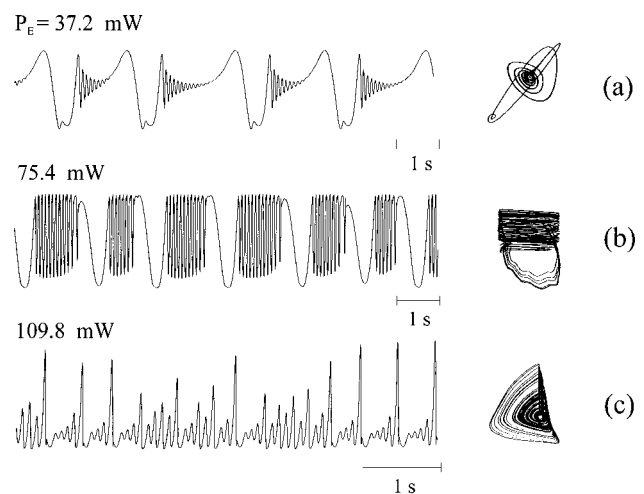


FIG. 3. Time evolutions and reconstructed attractors showing the basic kinds of three-dimensional dynamics observed in BOITAL cavities. (a) and (b) correspond to a two-layer device spaced with 140 and 540  $\mu\text{m}$  of glass and optical adhesive, respectively, but at different environment temperatures [25  $^\circ\text{C}$  for (a) and 18  $^\circ\text{C}$  for (b)]. The adhesive plays a twofold role responsible for the three-dimensional behavior of the two-layer device. (c) Corresponds to a three-layer device spaced with 140  $\mu\text{m}$ , 35  $\mu\text{m}$ , and 1 mm of glass, sunflower oil, and glass, respectively.

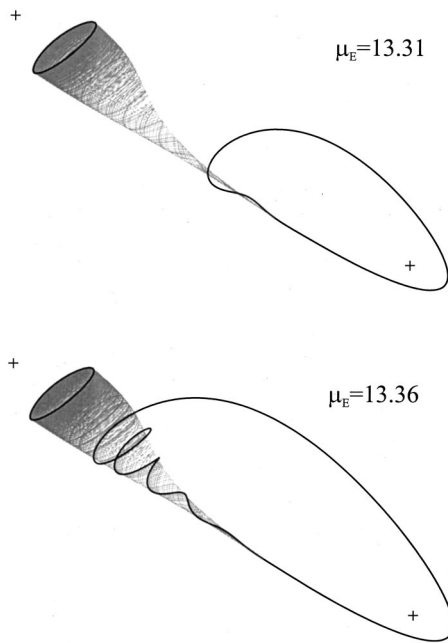


FIG. 4. Phase space representation of numerical results illustrating the nonlinear mixing of the oscillation modes associated with the Hopf bifurcations of a saddle-node pair of fixed points for  $N=3$ . The calculations correspond to the dimensionless physical parameters  $g_j=1,0,8,1$ ,  $\eta_j=1,-6.9,15.37$ ,  $k_j=D_j=1,0,1,1$ ,  $h_F=h_B=0.5$ ,  $j=1,2,3$ , whose definition and relation to the coefficients of Eqs. (1) are given in Ref. 14. The almost conical gray surface describes one side of the unstable manifold of the saddle limit cycle. The stable cycle has emerged from the node point for  $\mu_E=13.10$  and has grown without suffering any bifurcation up to  $\mu_E=13.36$ , but it has incorporated a number of helical turns around the saddle unstable manifold.

peaks before each outward spiraling. Thus underlying the dynamics there are homoclinic connections associated with saddle limit sets arising from the original saddle and node fixed points and having two- and one-dimensional stable manifolds, respectively. Under clear dominance of the first kind of homoclinicity, the system evolution describes Shil'nikov-type attractors,<sup>12</sup> while the other kind of homoclinicity produces Rössler-type folded bands.<sup>18</sup> In the parameter space, the variety of dynamics appears organized around the homoclinic cycle connecting the two kinds of saddle limit sets.

Figure 4 presents numerical results illustrating how the nonlinear mixing works in a Shil'nikov-type attractor for  $N=3$ . The initial node point has produced the stable cycle and now is a saddle focus with outgoing spiraling, while the initial saddle point has generated a saddle limit cycle by becoming fully unstable. One of the branches of the unstable manifold of the saddle limit cycle approaches the attracting cycle in a well-defined place. The spiral motion associated with the stable manifold of the saddle cycle affects the flow around the unstable manifold and works like a corkscrew on the stable limit cycle when it grows under the control parameter variation. The helical motion of the attractor evolves in time according to the oscillations of the saddle periodic orbit and mode mixing then occurs. The stable periodic orbit incorporates additional helical turns through a continuous deformation and, during the process, it can be involved in period-doubling and cyclic saddle-node bifurcations.<sup>19</sup> In

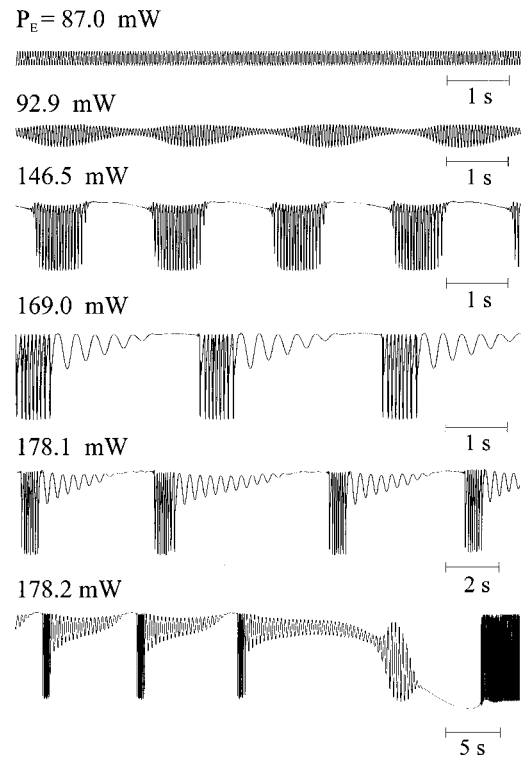


FIG. 5. Time evolutions observed in the reflected power of a four-layer BOITAL device for different incident light powers. The signals show how the two-frequency oscillation associated with an invariant torus is influenced by the attracting spiral of an external saddle focus.

this way, a complex attractor can develop together with a large number of nonstable periodic orbits and all of them will grow by transforming under the corkscrew effect up to being destroyed at the homoclinic bifurcation.

Figure 5 illustrates an experimental example of full instability behavior for  $N=4$ . The sequence of time evolutions for different incident light powers was obtained with a four-layer device of {glass-silicone-glass-sunflower oil} with thicknesses of 140, 35, 400, and 305  $\mu\text{m}$ , respectively. The fast oscillations shown for  $P_E=87\text{ mW}$  appeared through a supercritical Hopf bifurcation of a stable fixed point. The slow frequency modulation of the fast oscillations also appeared supercritically and it denotes the creation of a two-torus through a secondary Hopf bifurcation of the fast-frequency limit cycle. The stable torus grows with the input power by approaching the external saddle focus and a Shil'nikov-type dynamics is generated. The spiraling focus introduces oscillations at the intermediate frequency and, just before homoclinicity, the signal becomes aperiodic by showing a different number of such oscillations at the successive passages near the saddle. The process ends with the attractor destruction in the homoclinic bifurcation and the system then shifts to an oscillating state at the other side of the saddle separatrix, as evidenced by the transient signal for 178.2 mW.

Figure 6 corresponds to a very similar device as in the case of Fig. 5 but with a thinner layer of silicone, 30 instead of 35  $\mu\text{m}$ . This system generates the same oscillation frequencies but with the slower and faster oscillations appearing in the reverse order. For higher incident powers not

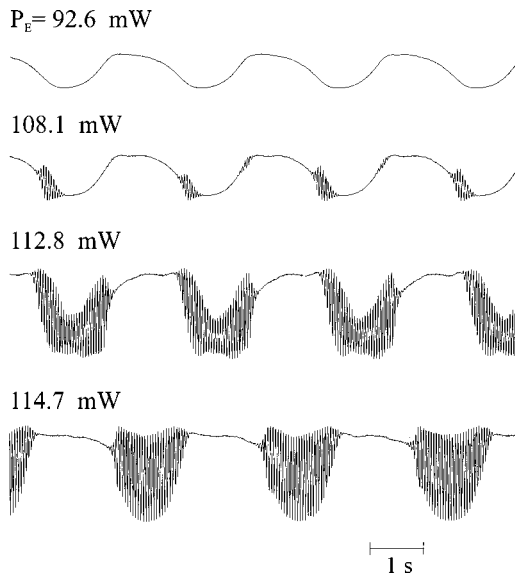


FIG. 6. Evolutions obtained with a four-layer device slightly different to that of Fig. 5. In this case the slow and fast oscillations appear in reverse order and the creation of an invariant torus does not seem likely. Intermediate frequency oscillations will appear also for higher incident powers.

shown in Fig. 6, the evolution incorporates the intermediate frequency of the external saddle focus and signals almost equal to those of Fig. 5 are obtained.

By considering the parameter space, it seems clear that the devices of Figs. 5 and 6 correspond to different sides of a codimension-two bifurcation of type  $(\pm i\omega_a, \pm i\omega_b)$ , in which the curves of two Hopf bifurcations of the same fixed point cross one another. The theory of universal unfoldings<sup>2</sup> shows that secondary Hopf bifurcations of the limit cycles can also emerge from this eigenvalue degeneracy and that, in first approximation, the two-frequency evolutions over the torus are based on the Hopf frequencies of the fixed point. The presence of an invariant torus is clear in the case of Fig. 5 but not so in the case of Fig. 6, where the fast oscillations emerge from nothing in two well-defined places of the slow-frequency limit cycle. Very similar time evolutions were numerically obtained from models (1) or (3) and the continuous following of the low-frequency limit cycle indicates that the localized packets of fast oscillations emerge without any local bifurcation. Thus a mechanism other than the torus bifurcation must be invoked in order to explain this kind of mode mixing, and Fig. 7 presents numerical results illustrating it. We are dealing with a four-dimensional phase space where an initially stable fixed point has done two successive Hopf bifurcations, and the saddle limit cycle created at the second bifurcation is now near to becoming stable by doing a sub-critical torus bifurcation.<sup>20</sup> In this situation, i.e., when the torus bifurcation will occur on the saddle limit cycle rather than on the stable one, the stable cycle exhibits a localized structure of helical motion in which the time dynamics evolves according the oscillations of the saddle limit cycle. In the case of Fig. 7 neither the stable orbit nor the saddle orbit have experienced any local bifurcation<sup>21</sup> and the helical motion (with the associated time dynamics) has appeared as a gradual deformation of the stable orbit during the control

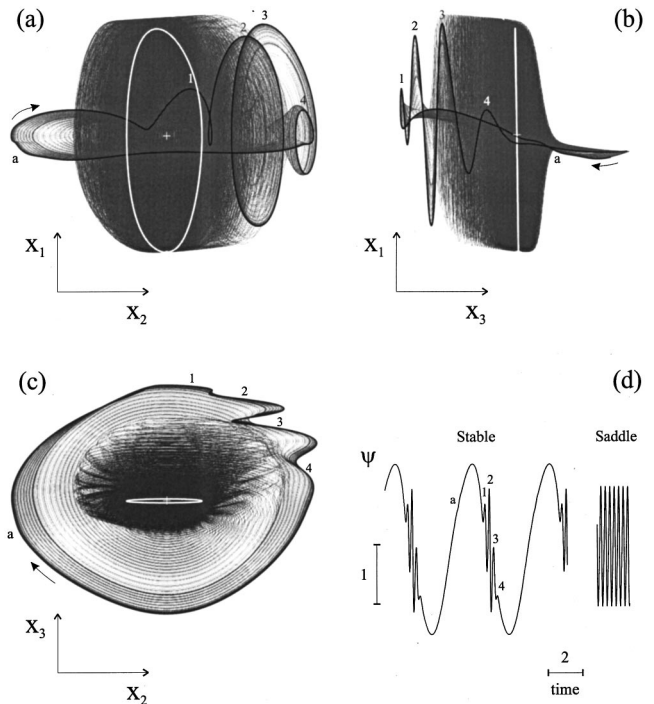


FIG. 7. Numerical results for  $N=4$  illustrating the nonlinear mode mixing of the two oscillation modes emerging in successive Hopf bifurcations of the same fixed point, for a situation in which the torus bifurcation will happen on the saddle orbit created at the second bifurcation. The black and white thick lines describe the stable and saddle periodic orbits, respectively, and the white cross denotes the fixed point. The unstable manifold of the saddle orbit is represented by means of a number of trajectories (Ref. 24) depicted by a thin black line. (a), (b), and (c) are projections in the planes defined by different pairs of variables. (d) presents the time evolution of the two periodic orbits. The unstable manifold is three-dimensional, while the stable manifold (not drawn) is two-dimensional and does not work like a separatrix. The numbers indicate certain places on the stable orbit, the same for the various representations. The label *a* denotes where a second helical structure will appear by increasing the control parameter. The calculations were done with model (3) for  $c_q = 50,438,98,480,71,358,22$ ,  $d_q = -17,601,66,044, -204,46,358,22$ ,  $q$  from 1 to 4, and  $\mu_E = 10$ . The Hopf bifurcations of the initially stable fixed point occurred for  $\mu_E = 8.2$  with angular frequency of 1.41, and  $\mu_E = 9.1$  with frequency of 25, respectively, and the torus bifurcation of the saddle orbit will occur for  $\mu_E = 10.3$  with the secondary frequency equal to 1.38.

parameter increase. The origin of this kind of mode mixing must be related to the influence of the flow dynamics of the saddle orbit toward a well-defined place of the stable orbit. It is worth remarking that a second structure of helical turns always appears on the stable orbit (in the zone denoted by *a* in Fig. 7) when the control parameter is increased, and the two structures usually connect together for higher control parameter values. This double structure can be appreciated in the experimental results of Fig. 6 and it constitutes a general feature also observed for higher dimensions (see the evolution for 66.3 mW in Fig. 8). On the other hand, in the case of Fig. 7, there is no influence of the external saddle fixed point because it is very far from its Hopf bifurcation. Nevertheless, in situations of full instability behavior, the attractor can exhibit the superposition of differently oriented helical structures associated with both the external and internal saddle limit sets. The time dynamics of the variable  $\psi$  typically exhibits the influence of the internal saddle sets in the two

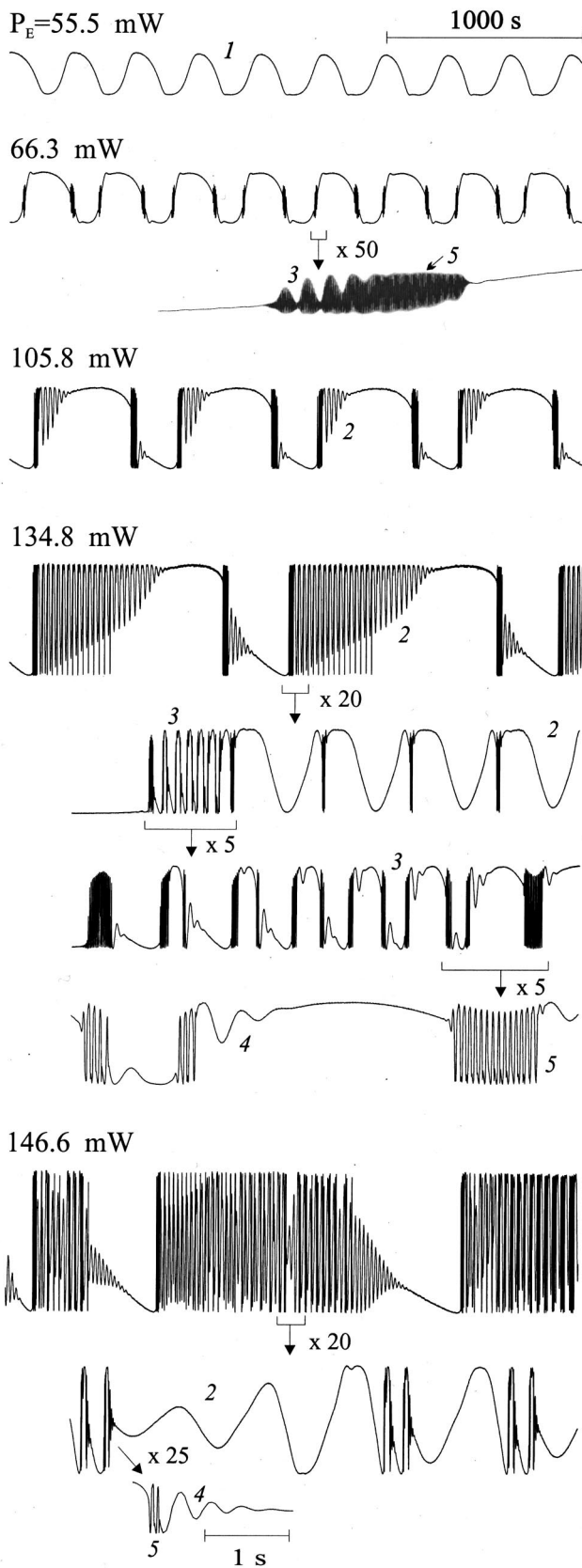


FIG. 8. Experimental time evolutions showing the nonlinear combination of five oscillation modes in the reflection of a BOITAL device with a five-layer spacer. The system exhibits six-dimensional dynamics because one of the layers introduces two degrees of freedom into the nonlinear feedback. The vertical and horizontal scales are common for all the signals, except for the time expanded details. The numbers in italics denote the different oscillation modes ordered from low to high frequency.

lateral sides of the lowest-frequency undulations, while the external saddle sets affect the top and the bottom.

Figure 8 presents really complex time evolutions that we interpret as corresponding to a six-dimensional dynamics. The recordings were obtained with a five-layer device of {glass-silicone-glass-gel-glass} with thicknesses of 140, 35, 400, 180, and 3000  $\mu\text{m}$ , respectively. The system was able to exhibit five oscillation modes supposedly because the gel layer introduced a double degree of freedom through the thermal expansion and thermo-optical effects. The five characteristic times determined when the oscillations appear nearly sinusoidal are 310, 23, 2.2, 0.35, and 0.07 s. The corresponding oscillation frequencies are denoted by  $\omega_j$ , with  $j$  from 1 to 5, and they are indicated in the figure by means of the number  $j$ . Notice that, in certain cases, the emergence of fast oscillations in the middle of a slower undulation may enlarge the corresponding characteristic time.

The signals for successive input light powers point out how the waveform structures appear. In the case of Fig. 8, the oscillations begin with a supercritical Hopf bifurcation at  $\omega_1$  on the node point, but soon incorporate two additional frequencies,  $\omega_3$  and  $\omega_5$ , in the two lateral structures appearing on each  $\omega_1$  undulation (see detail for 66.3 mW). The relation of the new frequencies with the node point cannot be verified in the experiment, but the analysis of the mathematical model shows that they emerge in successive Hopf bifurcations of this point by means of the corresponding saddle limit cycles. The numerical simulations indicate that evolutions like that for 66.3 mW appear without the occurrence of torus bifurcations on the stable cycle. The three-frequency waveform may be interpreted as the  $\omega_1$  stable limit cycle influenced by the out structures of either the pair of saddle periodic orbits or, more probably, a  $(\omega_3, \omega_5)$  saddle torus derived from one of these cycles. In other words, we conjecture a situation similar to that of Fig. 7, but for  $N=6$ , where a saddle two-torus has appeared in the center of the stable limit cycle and where the two-frequency motion of the saddle torus is transferred to certain places of the attractor as defined by the approach of the unstable manifold. In any case, the oscillations at  $\omega_1$ ,  $\omega_3$ , and  $\omega_5$  seem clearly associated with the node point and limit sets derived from it. The approach of the three-frequency attractor to the saddle point manifests first through the  $\omega_2$  oscillations appearing at the top of the  $\omega_1$  oscillations (105.8 mW). At higher powers the  $\omega_2$  oscillation mixes with the  $(\omega_3, \omega_5)$  structure while some  $\omega_4$  oscillations also appear (134.8 mW). The uniform amplitude of the  $\omega_1$ ,  $\omega_3$ , and  $\omega_5$  oscillations indicates the occurrence of the corresponding Hopf bifurcations, while the convergence of the  $\omega_2$  and  $\omega_4$  oscillations suggests that the saddle is even an attractive bifocus with a one-dimensional unstable manifold. The 146.6 mW signal indicates that the saddle point has already made the Hopf bifurcation at  $\omega_2$ . This is clearly denoted by the sporadic passages near the bifocus point with convergence at  $\omega_4$  and divergence at  $\omega_2$  (see detail for 146.6 mW). In addition, the large number of  $\omega_2$  oscillations with uniform amplitude suggests the presence of the saddle limit cycle and the relative proximity of its homoclinic connection. Homoclinic chaos may then be expected to occur in accordance with Shil'nikov's theorems<sup>22</sup>

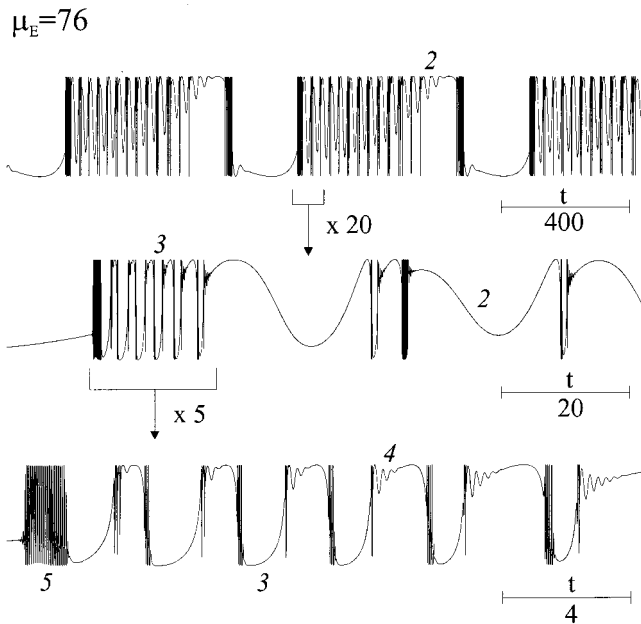


FIG. 9. Five-frequency oscillations numerically obtained from Eqs. (3) for  $N=6$ ;  $c_q=4.33, 7680, 76\ 400, 156\ 000, 11\ 500, 250$  and  $d_q=4.33, -766, 4280, -10\ 400, 276, -16.7$ , with  $q$  from 1 to 6,  $\psi^0=0$ , and  $\mu_E=76$ .

and, in fact, the waveform structure for 146.6 mW is not as repetitive as for lower light powers. Nevertheless, chaos is not the relevant thing in the signals of Fig. 8. What is remarkable is the degree of complexity and the robustness of these waveform structures and the presence of self-similarity features with respect to the time scale.

Figure 9 shows a numerical simulation obtained from system (3) for  $N=6$  and other parameters given in the caption. The  $c_q$  and  $d_q$  values have been determined by imposing the occurrence of three Hopf bifurcations on the node point at  $\mu_E=52.4, 58.2,$  and  $58.3$ , with angular frequencies equal to 0.02, 125, and 2.98, respectively, and two Hopf bifurcations on the saddle point at  $\mu_E=64.7$  and  $104.6$ , with frequencies 0.25 and 24.9, respectively. The time evolution of Fig. 9 represents the reflected power for  $\mu_E=76$  and its structure is really similar to that of the 134.8-mW signal of Fig. 8. The dimensionless characteristic times contained in the numerical evolution are 721, 25, 2.6, 0.26, and 0.05, and the corresponding angular frequencies are  $\omega_j=0.009, 0.25, 2.4, 24,$  and  $125, j=1, \dots, 5$ , which must be compared to the Hopf frequencies. The numerical simulations confirm that the attractor evolves around an unstable fixed point that has effectively performed three successive Hopf bifurcations at the imposed  $\mu_E$  values and with the preselected oscillation frequencies. The three Hopf frequencies of the node are similar to the  $\omega_1, \omega_5,$  and  $\omega_3$  of the numerical evolution, respectively.  $\omega_5$  is precisely equal to the Hopf frequency and the slower values of  $\omega_1$  and  $\omega_3$  can be attributed to the presence of intermediate faster oscillations. On the other hand, the attractor visits the neighborhood of a saddle point that has performed one Hopf bifurcation and is even far from the second bifurcation. These Hopf frequencies are very similar to the  $\omega_2$  and  $\omega_4$  of the time evolution. Thus the five frequencies contained in the numerical signal are clearly related

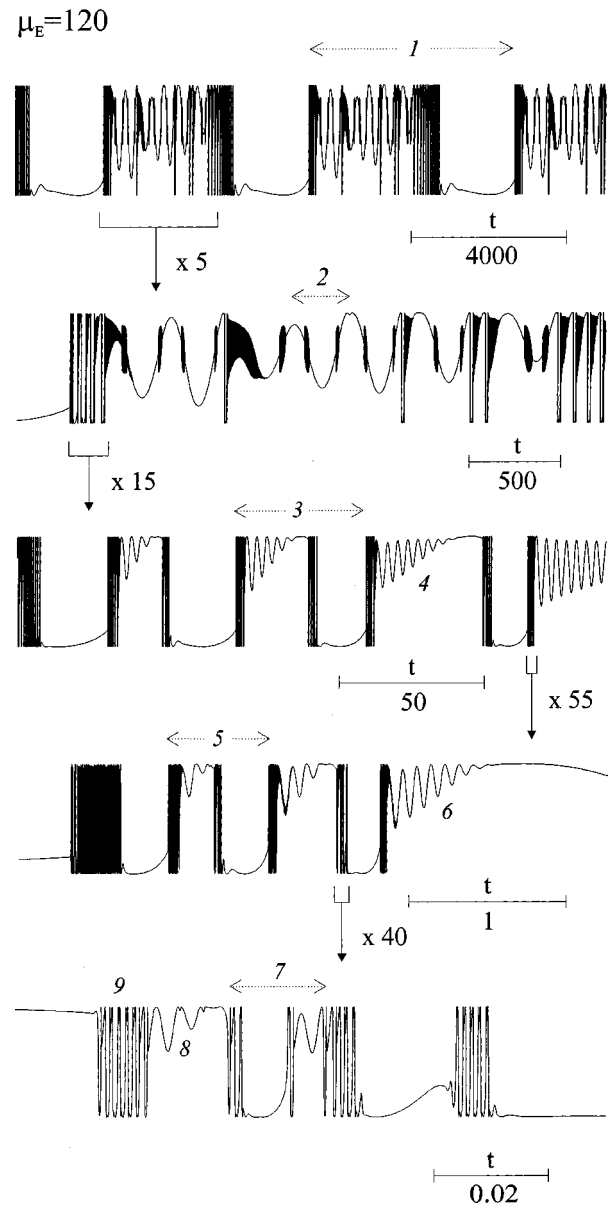


FIG. 10. Numerical evolution for  $N=10$  obtained from Eqs. (3) by imposing five Hopf bifurcations on the node point with angular frequencies 0.002, 0.2, 12, 350, and 6000, and four bifurcations on the saddle point with frequencies 0.02, 1.8, 70, and 1500. The waveform evolution shows the nonlinear combination of nine oscillation modes whose frequencies are similar to the Hopf values.

to the Hopf instabilities of the saddle-node pair of fixed points.

A wider perspective may be achieved by analyzing the full instability behavior of higher-dimensional systems and, with this aim, we present a numerical example for  $N=10$  in Fig. 10. The dynamical system has been designed by imposing five Hopf bifurcations on the node point and four bifurcations on the saddle point. For  $\mu_E=120$ , the node point is fully unstable, while the saddle point has done only one bifurcation and is near to doing the other three bifurcations. The time evolution shows the nonlinear mixing of nine oscillation modes. The odd label modes are associated with the

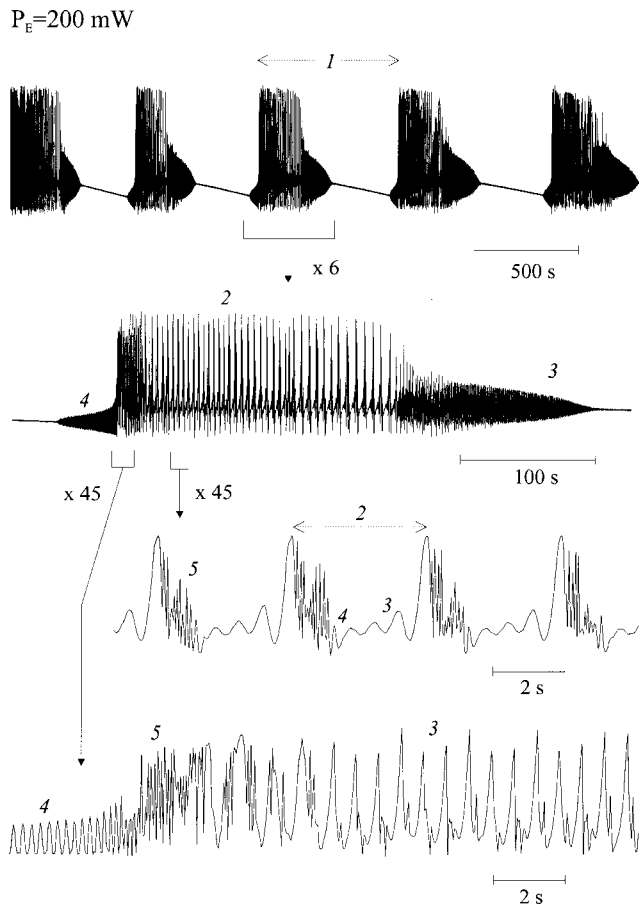


FIG. 11. Experimental example of a time evolution illustrating a six-dimensional dynamics with a waveform structure based on five oscillation modes that looks very different to the signals of Figs. 8–10.

Hopf bifurcations of the node point and the even labels correspond to the saddle point. Self-similarity is clearly seen in the successive zooms of Fig. 10 and it is worth noticing that the oscillations associated with either the node or the saddle maintain their roles along the similarity scale.

Experiments and numerical simulations with different multilayer structures indicate that the full instability behavior of the BOITAL systems manifests most generically with time evolutions like those of Figs. 8–10, where the oscillation frequencies associated with either the node or the saddle fixed points clearly play different roles. Nevertheless, qualitatively different complex waveforms can also be observed for reduced parameter ranges. For instance, Fig. 11 shows an example obtained with a five-layer device similar to that of Fig. 8 but with a thinner layer of gel, 160 instead of 180  $\mu\text{m}$ . The signal contains five characteristic times of 550, 3.8, 0.7, 0.25, and 0.1 s, respectively, and the nonlinear mixing produces a rather irregular waveform where the roles of the different oscillation modes do not appear so clearly defined. The numerical studies suggest the association of the observed nongeneric behaviors with the proximity of particular eigenvalue degeneracies sustaining codimension-two bifurcations. For instance, the evolutions of Fig. 11 may be related with a degeneracy of type  $(0, \pm i\omega)$  because signals of this type are numerically obtained when one of the Hopf

bifurcations of a fixed point is approached toward the turning point of a saddle-node bifurcation.

#### IV. DISCUSSION AND CONCLUSIONS

First of all let us remark that the BOITAL systems exhibit the full instability behavior with two peculiar features: (i) the various oscillation frequencies are rather different inasmuch as they appear roughly scaled for successive orders of magnitude, and (ii) when ordered according to their values, the different frequencies appear alternatively associated with either the node or the saddle point and the lowest frequency always corresponds to the node. These peculiarities occur because (a) the characteristic times of a given system are associated with the heat diffusion from the localized source to the various layers of the cavity spacer, and (b) the dynamical variables participate in the nonlinear feedback through a linear combination of them. For instance, numerical simulations with the same model but for nonphysical parameter values yielding more similar oscillation frequencies indicate significant changes in the observed full instability behaviors, and it is then important to stress that our discussion here is based on situations like those of the BOITAL systems.

The irregular succession of undulations of different frequencies forming the full instability waveforms usually repeat with regularity and even periodically. This fact indicates that the high degree of instability represents a way toward creating irregular and complex evolutions independent of chaos. In fact, chaos was rarely found during our numerical simulations and the higher the number of oscillation modes the more pronounced the absence of chaos. This is really surprising because, according to our interpretation, the development of the fully unstable behavior underlies a variety of saddle connections and chaos would then be reasonably expected.

The waveform structures of the full instability behavior are very robust in the sense that they change slowly with the control parameter. In other words, the full instability behavior is a coarse phenomenon occurring continuously in the parameter space regions where several Hopf bifurcations of the fixed points appear relatively close. This makes another distinction with respect to chaos, and it explains why a method exclusively based on the linear stability analysis of the fixed points can be enough for designing fully unstable  $N$ -dimensional systems.<sup>10</sup>

The nonlinear mechanisms responsible for the full instability waveforms introduce irregularity by affecting both the relative phases and amplitudes of the oscillation modes in a complex manner. At the same time, however, the similarity features typically found in the time evolutions indicate an intrinsic organization of the mode mixing mechanism around the saddle-node pair of fixed points. The nonlinear mode mixing may be considered as a global process affecting the flow of the phase space region where the complex structure of interrelated invariant sets will be created. The process is triggered by the Hopf bifurcations of the fixed points, but it is organized by the global structure of invariant manifolds of the different saddle limit sets, which underlie a variety of

possible homoclinic and heteroclinic connections. The mode mixing happens through a continuous deformation of the flow in particular zones of the attractor and, although it may be accompanied by complex bifurcational sequences, only the bifurcations yielding invariant tori participate directly in the mode mixing. Other bifurcations involving periodic orbits, like the period-doubling, cyclic saddle-node, and homoclinic bifurcations, do not contain intrinsic mechanisms for the definition of a new characteristic frequency and they cannot induce mode mixing.

The occurrence of torus bifurcations seems likely in the fully unstable systems because these systems appear in the parameter space relatively close to the loci of eigenvalue degeneracies of the type  $(\pm i\omega_1, \pm i\omega_2, \dots, \pm i\omega_q)$ , in which  $q$  Hopf bifurcations happen simultaneously on the same fixed point, and because it is reasonable to suspect that a variety of torus bifurcations can emerge from each one of such degeneracies.<sup>23</sup> The Landau sequence of consecutive bifurcations yielding a stable high-dimensional torus is in principle possible, but we suspect that the corresponding parameter space domain is rather restricted and probably very close to the corresponding high-order degeneracy. It seems more likely the occurrence of different low-dimensional tori created from the different limit cycles emerged from the fixed point. On the other hand, a given limit cycle can perhaps generate successive two-tori with different secondary frequencies, like a fixed point can produce successive limit cycles, and the same might happen with the low-order tori. It seems not possible, however, that different limit cycles generate simultaneously sequences of torus bifurcations with the same set of frequencies. For instance, for  $N=4$ , the universal unfoldings of  $(\pm i\omega_1, \pm i\omega_2)$  show that only one of the two limit cycles emerging from a node point can do the secondary bifurcation at the frequency of the other cycle but not the two cycles at once.<sup>2</sup>

The important point for the full instability behavior is that the limit cycle that does not do the torus bifurcation can also incorporate an oscillatory component at the other frequency through the mixing mechanism discussed above. And the other important point is that not only one fixed point but a set of them, related by saddle-node bifurcations, can participate together in the generation and mixing of oscillation modes. These elements constitute the generalized Landau scenario where the full instability behavior develops.

The full instability behavior has been investigated in particular classes of dynamical systems and it is then necessary to ask how general the phenomenon is. According to our interpretation, we find reason to suspect that the occurrence of the several Hopf bifurcations in a small enough parameter domain will be generically associated with the development of nonlinear mechanisms of mode mixing. Nevertheless, the complexity of the process and the time dynamics features will probably change with the actual properties of the nonlinear vector field. Particularly relevant may be the values of the oscillation frequencies, as well as the order of occurrence of the bifurcations on the fixed points. On the other hand, the high degree of instability behavior of vector fields possessing multidimensional arrays of fixed points, instead of a simple saddle-node pair, will probably produce rather different re-

sponses. Such complex structures of fixed points can occur for vector fields based on several linearly independent nonlinear functions, such as, for instance, the case of a set of coupled nonlinear oscillators.

Another question is which classes of systems are compatible with the full unstable behavior and how can their parameters be adjusted to achieve that behavior. In principle, the situations of full instability could be identified by means of the linear stability analysis of the steady-state solution. Nevertheless, in general, it is not easy to establish the corresponding conditions for a given multiparameter family of  $N$ -dimensional systems and this probably explains why the full instability behavior has not already been observed. We have shown<sup>10</sup> that this analysis is feasible for systems based on vector fields whose nonlinear part is a scalar-valued nonlinear function of a single variable that, in its turn, is a linear combination of the  $N$  dynamic variables, i.e., systems in the form (3) with an arbitrary nonlinear function  $A(\psi)$ . In this case, the linear stability analysis allows us to design the system in order to obtain  $N-1$  Hopf bifurcations on a saddle-node pair of fixed points with preselected values for the frequency and control parameter.

From the phenomenological point of view it is worth noting that we have found the full instability behavior in the BOITAL devices because they enable us to have a simple and effective criterion for properly choosing the set of parameters. In practice, we select the multilayer properties by trying to see if the alternatively opposite effects of the various layers tend to mutually compensate. In other words, we attempt to achieve a relative equilibrium among the competitive participation of the various degrees of freedom into the nonlinear mechanisms. The rule is useful for both the experiment and the physical model based on the heat equation and allows us to derive proper sets of coefficients for the reduced  $N$ -order model of Eqs. (1).

A high degree of Hopf instability behavior requires a large number of variables participating into the nonlinear feedback by driving competitive effects of different characteristic times. These intrinsic features of the BOITAL devices may be present in other real-world systems, specially those with a profusion of self-oscillatory processes. The oscillatory behavior is perhaps the most typical response of the evolutionary systems found in biology, economy, ecology, and sociology. Such oscillations have probably appeared in the course of the system development driven by the interaction with the environment. Extending such a view, we can imagine adaptive systems developing toward exhibiting high-instability states, and this would be in reality the case if such states would be useful for the existence of the system in the middle of its surroundings.

## ACKNOWLEDGMENTS

The authors are indebted to J. I. Rosell, F. Boixader, and R. Pons for their significant contributions in the development and understanding of the BOITAL systems. This work was supported by the Spanish DGES under Grant No. PE98-0899.

- <sup>1</sup>*Dynamic Biological Networks*, edited by R. M. Harris-Warrick, E. Marder, A. I. Selverton, and M. Moulins (MIT Press, Cambridge, 1992).
- <sup>2</sup>See, e.g., J. Guckenheimer and P. Holmes, *Nonlinear Oscillations, Dynamical Systems, and Bifurcations of Vector Fields* (Springer, New York, 1983); S. Wiggins, *Introduction to Applied Nonlinear Dynamical Systems and Chaos* (Springer, New York, 1990).
- <sup>3</sup>L. D. Landau, C. R. (Dokl.) Acad. Sci. USSR **44**, 311 (1944), reproduced in *Chaos II*, edited by Hao Bai-Lin (World Scientific, Singapore, 1990), p. 115.
- <sup>4</sup>The torus bifurcation does not permit the superposition with arbitrary phase assumed by Landau in relation to the occurrence moment of the secondary instability.
- <sup>5</sup>See, e.g., *Hydrodynamic Instabilities and the Transition to Turbulence*, edited by H. L. Swinney and J. P. Gollub (Springer-Verlag, Berlin, 1981).
- <sup>6</sup>D. Ruelle and F. Takens, Commun. Math. Phys. **20**, 167 (1971); S. Newhouse, D. Ruelle, and F. Takens, *ibid.* **64**, 35 (1978).
- <sup>7</sup>Half of the bifurcations occur on each point, if  $N$  is odd, while one bifurcation more happens on the initially stable point, if  $N$  is even.
- <sup>8</sup>A sequence of torus bifurcations initiated from a fixed point is intrinsically related to the successive Hopf bifurcations of that point and the corresponding oscillations are usually based on the same frequencies.
- <sup>9</sup>In fact, only one attractor can emerge from the variety of Hopf bifurcations of a saddle-node pair of fixed points but additional attractors may arise from secondary processes.
- <sup>10</sup>J. Rius, M. Figueras, R. Herrero, F. Pi, G. Orriols, and J. Farjas, Phys. Rev. E **62**, 333 (2000).
- <sup>11</sup>G. Orriols, C. Schmidt, and F. Pi, Opt. Commun. **63**, 66 (1987).
- <sup>12</sup>R. Herrero, R. Pons, J. Farjas, F. Pi, and G. Orriols, Phys. Rev. E **53**, 5627 (1996).
- <sup>13</sup>J. I. Rosell, J. Farjas, R. Herrero, F. Pi, and G. Orriols, Physica D **85**, 509 (1995).
- <sup>14</sup>J. Farjas, J. I. Rosell, R. Herrero, R. Pons, F. Pi, and G. Orriols, Physica D **95**, 107 (1996).
- <sup>15</sup>S. L. McCall, Appl. Phys. Lett. **32**, 284 (1978); H. M. Gibbs, S. S. Tang, J. L. Jewell, D. A. Weinberger, and K. Tai, *ibid.* **41**, 221 (1982).
- <sup>16</sup>H. J. Kong and W. Y. Hwang, J. Appl. Phys. **67**, 6066 (1990).
- <sup>17</sup>J. I. Rosell, F. Pi, F. Boixader, R. Herrero, F. Farjas, and G. Orriols, Opt. Commun. **82**, 162 (1991).
- <sup>18</sup>R. Herrero, F. Boixader, G. Orriols, J. I. Rosell, and F. Pi, Opt. Commun. **113**, 324 (1994).
- <sup>19</sup>P. Glendinning and C. Sparrow, J. Stat. Phys. **35**, 645 (1984).
- <sup>20</sup>The two-dimensional eigenspace and the oscillation frequency of the secondary Hopf bifurcation of the saddle cycle are directly related to those of the first Hopf bifurcation of the fixed point. This implies that the secondary bifurcation will be subcritical.
- <sup>21</sup>This has been verified by continuously following both periodic orbits.
- <sup>22</sup>L. P. Shil'nikov, Int. J. Bifurcation Chaos Appl. Sci. Eng. **4**, 489 (1994).
- <sup>23</sup>The possibilities of invariant tori generation through sequences of bifurcations initiated from a fixed point are not well known. The theory of universal unfoldings developed for certain low-dimensional degeneracies (Ref. 2) gives precise information for  $N$  up to 4, but only some general ideas may be tentatively extrapolated to higher dimensional problems.
- <sup>24</sup>Eighty trajectories initiated from different points of the unstable eigenspace of the saddle cycle. The proximity of the initial point to the saddle orbit is chosen such that the error due to the separation between the eigenspace and the invariant manifold is of the same order as the error of the numerical integration. The initial points are taken in 10 temporally equidistant places along the orbit and with 8 different output angles within the two-dimensional eigenspace transverse to the orbit.